A Direct Force Probe for Measuring Mechanical Integration Between the Nucleus and the Cytoskeleton

Qiao Zhang, **Andrew Tamashunas**, and **Tanmay P. Lele**

Department of Chemical Engineering, University of Florida, Gainesville, FL, United States

Qiao Zhang: qzhang02@ufl.edu; Andrew Tamashunas: atamash@ufl.edu

Abstract

The mechanical properties of the nucleus determine its response to mechanical forces generated in cells. Because the nucleus is molecularly continuous with the cytoskeleton, methods are needed to probe its mechanical behavior in adherent cells. Here, we discuss the direct force probe (DFP) as a tool to apply force directly to the nucleus in a living adherent cell. We attach a narrow micropipette to the nuclear surface with suction. The micropipette is translated away from the nucleus, which causes the nucleus to deform and translate. When the restoring force is equal to the suction force, the nucleus detaches and elastically relaxes. Because the suction pressure is precisely known, the force on the nuclear surface is known. This method has revealed that nano-scale forces are sufficient to deform and translate the nucleus in adherent cells, and identified cytoskeletal elements that enable the nucleus to resist forces. The DFP can be used to dissect the contributions of cellular and nuclear components to nuclear mechanical properties in living cells.

Keywords

INTRODUCTION

Pathologies such as cancer involve alterations to nuclear shape and structure[1,2], which are generally accompanied by a 'softening' of the nucleus[3,4]. Nuclear resistance to mechanical deformation has been generally characterized by applying a force to isolated nuclei[5].

The nucleus in cells is molecularly connected to the cytoskeleton by the Linker of Nucleoskeleton and Cytoskeleton (LINC) complex[6–9]. As a result, the nucleus is mechanically integrated with the cytoskeleton and, through cell-substratum adhesions, the extracellular matrix. Mechanically probing the nucleus inside adherent cells can provide insight into this mechanical integration. Methods to manipulate nuclei in living cells include micropipette aspiration[10,11], and atomic force microscopy[12–14]. We recently described a

direct force probe (DFP) that applies mechanical forces directly on the nucleus in a living adherent cell[15].

Here, we outline the procedure for using a microinjection system that is commonly available in microscopy facilities to apply a known, nano-scale mechanical force directly to the nucleus in an adherent cell. A femtotip (0.5 μm diameter micropipette tip) is mounted and connected to the microinjection system by a tube. The tip, positioned at a 45° angle relative to the surface of the culture dish, is lowered until adjacent to the nuclear surface. The tube is then disconnected and opened to the atmosphere, which creates a negative suction pressure on the nuclear surface and seals the micropipette tip against the nuclear surface. Through translation of the micropipette tip, the nucleus is deformed and eventually (depending on the magnitude of force applied), detached from the micropipette. This detachment occurs when the restoring (resisting) forces, exerted by the nucleus and cell, equal the suction force applied by the micropipette. Analysis can be performed by measuring the displacement of the nucleus, the length strain (Equation 1), or the area strain (Figure 1A).

PROTOCOL

1. Preparing Cells for Imaging

Note: The direct force probe (DFP) can be used for any adherent cell type. Here, NIH 3T3 mouse fibroblasts are used as the model cell line for this protocol.

1.1 Culture NIH 3T3 fibroblast cells in Dulbecco's Modified Eagle's Medium (DMEM) supplemented with 10% donor bovine serum and 1% Penicillin-Streptomycin on a 35-mm glass bottom dish until desired confluency. Maintain cells at 37 °C and 5% CO_2.

1.1.1 Be sure to coat all 35-mm glass bottom dishes with 5 μg/mL of fibronectin (or similar ECM protein), before seeding NIH 3T3 cells for imaging.

Note: The cells must be fully spread and adherent on the dish for the experiment. There are not any constraints in terms of confluency for the DFP method to work.

1.2 Immediately prior to the experiment, wash the cells twice with PBS followed by a single wash with complete growth medium.

1.3 Add 3 mL of complete growth medium to the glass bottom dish.

2. Microscopy and Image Acquisition

Note: An inverted fluorescence microscope (or equivalent) with micromanipulator installed to the side arm, according to the manufacturer's recommendations. The microscope should also be outfitted with an environmental chamber to maintain the temperature at 37 °C, and CO_2 level at 5%. A micromanipulator and microinjector attached to the microscope is also required. An oil immersion 40x/1.3 NA or 60x/1.49 NA (or equivalent objectives) are recommended for the experiments. The microscope should be mounted on a vibration isolation table.

2.1 Turn on the microinjector per the manufacturer's protocol.

2.2 Using an immersion oil dropper, apply a single drop of immersion oil on top of the objective lens.

2.3 Clamp the dish tightly into the dish holder and load the dish holder onto the stage.

Note: The cells must be maintained at 37 °C and 5% CO_2 throughout the experiment.

2.4 Adjust the height of the objective to bring the cells into focus (**Plane A,** Figure 1B).

2.5 Move the microscope stage to find a cell of interest.

2.6 Rotate the joystick on the micromanipulator to move the pipet holder to the top position. Load the 0.5 μm diameter tip micropipette onto the pipet holder.

2.6.1 To avoid cell adhesion to the micropipette, pre-treat the micropipette tip with 0.3 mg/mL PLL-g-PEG solution for 1 h at room temperature. Test for adhesion by touching the micropipette to the nucleus without any suction pressure, and then translating the micropipette away from the nucleus. The absence of adhesion can be discerned from a complete lack of nuclear deformation and translation.

Note: Please follow manufacture suggestions to open the package.

2.7 Raise the objective focal plane above Plane A and the top of the cell to Plane B by adjusting the fine control (Figure 1B, see step 2.4).

2.8 Set the micromanipulator to **Coarse** control. Slowly bring the micropipette down to Plane B by watching for the silhouette of the micropipette, until the micropipette comes fully into focus.

2.9 Once the micropipette tip is in focus, set the micromanipulator to **Fine** control.

2.10 Lower the objective to the equatorial plane of the cell (Plane A, Figure 1B) and lower the micropipette to around 15 μm above Plane A (Figure 1B, dashed micropipette).

2.11 Set the compensation pressure (P_c) on the microinjector to desired pressure; wait several seconds for the pressure to stabilize.

Note: The optimal pressure set point depends on both cell type and the specific goals of the experiment. For most cases, 300 hPa would be a good starting point.

2.12 Ensure that the micropipette is not clogged by using the **Clean** setting on the micromanipulator panel and checking to make sure air bubbles emerge from the micropipette tip.

2.13 Insert the tip into the cell by gradually lowering the micropipette until the tip is lightly touching the nuclear surface.

Note: When lowering the micropipette, the silhouette of the micropipette tip will become clear as it comes into focus. Before the micropipette touches the nucleus, raise the objective focus and align the micropipette tip with nucleus

(same x-y coordinate, higher z-plane). Return the focus back to the equatorial plane of the nucleus (Plane A, Figure 1B) and gradually lower the micropipette tip.

2.14   Create a seal between the micropipette tip and the nuclear membrane by disconnecting the pressure-supply tube from the microinjection system, thereby opening the end of the micropipette tube to the atmosphere. This step creates a negative pressure equal to P_c on the nuclear surface.

2.15   Acquire images with the microscopes image collection software. Set up an avi-acquisition (video) or nd-acquisition (images) in the image collection software.

2.15.1 For any imaging acquiring software, set up real-time video imaging or time-lapse image acquisitions with a short time interval.

2.16   Toggle to the corresponding fluorescent imaging channel (*i.e.,* GFP, RFP, *etc.*) and begin imaging.

2.17   Translate the micropipette tip away from the body of the cell (to the right, Figure 1B) until the nucleus detaches from the micropipette.

Note: Pull the tip along the positive x-direction (to the right in the field of view). The pulling rate can be programmed and controlled by computer or the joystick can be moved manually. We have not found any correlation between the pulling rate and nuclear deformation[15] suggesting a primarily elastic response to force.

3. Data Analysis

3.1   Perform image analysis with any basic image-processing software available. The extent of nuclear deformation can be quantified by either the length strain (ε) or the area strain (Fi**gure 1A**). Quantify length strain using Equation 1, where L and L_0 represent the lengths of the nucleus at maximum deformation and the initial position, respectively.

$$\varepsilon = \frac{L}{L_0} - 1 \quad \text{(Equation 1)}$$

REPRESENTATIVE RESULTS

Figure 2A shows the forcing of an NIH 3T3 mouse fibroblast nucleus. As the micropipette tip is translated to the right, the nucleus deforms and eventually detaches from the micropipette tip. The length strain of the nucleus is seen to increase with increasing suction force (Figure 2B). The front edge of the nucleus (micropipette pulling edge) forms a nuclear protrusion and the trailing edge is displaced from its original position. The length of protrusion is much greater than the trailing edge displacement (Figure 2C), suggesting a tight integration between the nucleus and the surrounding cytoplasm. The time scales are short for relaxation of the nuclear front edge (<1 s), and the nuclear back edge (<2 s) (Figure 2D).

We have used the DFP method to determine how cytoskeletal forces contribute to nuclear resistance to deformation in the cell. While no significant differences in nuclear deformation or translation were found after F-actin (by cytochalasin-D) or microtubule disruption (by nocodazole), reducing vimentin expression through siRNA-based knockdown resulted in significantly greater nuclear translation and deformation (Figure 3). This suggests that vimentin intermediate filaments in fibroblasts are the main cytoskeletal element that help the nucleus resist local force.

DISCUSSION

Measuring the mechanical integration of the nucleus with the cytoskeleton is a challenge for most current methods, such as micropipette aspiration[16], because they require either isolated nuclei (where the nucleus is decoupled from the cytoskeleton) or nuclei in suspended cells (where extracellular forces, such as traction forces, are absent). Force has been applied to the nucleus by applying biaxial strain to cells adherent to a membrane[17,18]; however, this technique is limited by the fact that the force on the nucleus is unknown. Atomic force microscopy (AFM) probes have been used to indent the nucleus in intact cells; these offer the advantage that they reveal the mechanical properties of the nucleus while it is integrated with the cytoskeleton. To add to existing *in vivo* techniques for characterizing the nucleus[12–14], we have developed a simple and robust method to mechanically probe the nucleus in a living adherent cell while it remains integrated to the surrounding cytoskeleton. A key feature of this technique is that the force on the nucleus is precisely known and controlled.

By applying the DFP, we estimate that nano-newton scale forces are sufficient to deform and translate the nucleus in living, adherent cells. Furthermore, through systematic studies of the contributions of various cytoskeletal elements, we have found that vimentin-based intermediate filaments are the primary component of the cellular cytoskeleton responsible for stiffening the nucleus in the cell [15].

Some caveats apply with these experiments. It is important to regularly check the micropipette tip for clogging or breakage during experiments, as both clogging of the micropipette or fracture of the tip would cause unknown changes to the suction pressure applied on the cell. To check if the micropipette is clogged, use the **Clean** setting on the manipulator to apply maximum pressure and check for air bubbles emerging from the micropipette tip. If the micropipette tip is broken or fractured, replace the micropipette before beginning the next experiment. Also, it is important to confirm that the nuclear strain varies with the force, and is zero at zero force (see Neelam *et al.*[15]). If this is not observed in experiments, then it is possible that non-specific adhesion between the micropipette tip and the nuclear surface (despite treatment with PLL-PEG) may be responsible for nuclear deformation. Another limitation of the technique is that insertion of the micropipette into the cell itself may cause some local disruption of cytoskeletal structures.

It is useful to test for correlations between the extent of nuclear deformation/translation and loading rate. An absence of correlation would imply a primarily elastic resistance. Indeed, this is what we have found to be the case for fibroblast nuclei[15]. While the force on the

nucleus is known, the method does not allow the calculation of parameters like the Young's modulus. We have primarily used it to dissect contributions of cellular structures to the resistance to nuclear deformation and translation in the cell. While we have reported two-dimensional nuclear shapes[15,19], it may be useful to quantify the full three-dimensional shape of the nucleus under force.

The suction pressure in the micropipette is known, but it is larger than the actual pressure applied to the nuclear surface due to flow of water through pores[10]. However, we have shown that the resistance to flow through the nuclear pores is much larger through the micropipette (see supporting information for calculations in Neelam *et al.*[15]) for reasonable membrane permeabilities and micropipette dimensions. Therefore, the pressure at the outer membrane surface should be equal to the suction pressure despite the existence of flow.

In conclusion, the DFP allows the user to quantify the mechanical response of the integrated nucleus-cytoskeleton in an adherent cell to a known and controlled force. This method could be used to dissect the contributions of molecular components in the nucleus and in the cytoplasm to the mechanical behavior of the nucleus within the cell.

Acknowledgments

References

1. Chow KH, Factor RE, Ullman KS. The nuclear envelope environment and its cancer connections. Nature Reviews Cancer. 2012; 12(3):196–209. DOI: 10.1038/nrc3219 [PubMed: 22337151]

2. Zink D, Fischer AH, Nickerson JA. Nuclear structure in cancer cells. Nature Reviews Cancer. 2004; 4(9):677–687. DOI: 10.1038/nrc1430 [PubMed: 15343274]

3. Bank EM, Gruenbaum Y. The nuclear lamina and heterochromatin: a complex relationship. Biochemical Society Transactions. 2011; 39(6):1705–1709. DOI: 10.1042/BST20110603 [PubMed: 22103511]

4. Lammerding J, et al. Lamins A and C but not lamin B1 regulate nuclear mechanics. Journal of Biological Chemistry. 2006; 281(35):25768–25780. DOI: 10.1074/jbc.M513511200 [PubMed: 16825190]

5. Dahl KN, Engler AJ, Pajerowski JD, Discher DE. Power-law rheology of isolated nuclei with deformation mapping of nuclear substructures. Biophysical Journal. 2005; 89(4):2855–2864. DOI: 10.1529/biophysj.105.062554 [PubMed: 16055543]

6. Crisp M, et al. Coupling of the nucleus and cytoplasm: role of the LINC complex. Journal of Cell Biology. 2006; 172(1):41–53. DOI: 10.1083/jcb.200509124 [PubMed: 16380439]

7. Sosa BA, Rothballer A, Kutay U, Schwartz TU. LINC complexes form by binding of three KASH peptides to domain interfaces of trimeric SUN proteins. Cell. 2012; 149(5):1035–1047. DOI: 10.1016/j.cell.2012.03.046 [PubMed: 22632968]

8. Tapley EC, Starr DA. Connecting the nucleus to the cytoskeleton by SUN-KASH bridges across the nuclear envelope. Current Opinion in Cell Biology. 2013; 25(1):57–62. DOI: 10.1016/j.ceb.2012.10.014 [PubMed: 23149102]

9. Arsenovic PT, et al. Nesprin-2G, a Component of the Nuclear LINC Complex, Is Subject to Myosin-Dependent Tension. Biophysical Journal. 2016; 110(1):34–43. DOI: 10.1016/j.bpj.2015.11.014 [PubMed: 26745407]

10. Rowat AC, Lammerding J, Ipsen JH. Mechanical properties of the cell nucleus and the effect of emerin deficiency. Biophysical Journal. 2006; 91(12):4649–4664. DOI: 10.1529/biophysj.106.086454 [PubMed: 16997877]

11. Rowat AC, Foster LJ, Nielsen MM, Weiss M, Ipsen JH. Characterization of the elastic properties of the nuclear envelope. Journal of the Royal Society Interface. 2005; 2(2):63–69. DOI: 10.1098/rsif. 2004.0022

12. Pagliara S, et al. Auxetic nuclei in embryonic stem cells exiting pluripotency. Nature Materials. 2014; 13(6):638–644. DOI: 10.1038/nmat3943 [PubMed: 24747782]

13. Liu H, et al. In situ mechanical characterization of the cell nucleus by atomic force microscopy. ACS Nanotechnology. 2014; 8(4):3821–3828. DOI: 10.1021/nn500553z

14. Krause M, Te Riet J, Wolf K. Probing the compressibility of tumor cell nuclei by combined atomic force-confocal microscopy. Physical Biology. 2013; 10(6):065002. [PubMed: 24304807]

15. Neelam S, et al. Direct force probe reveals the mechanics of nuclear homeostasis in the mammalian cell. Proceedings of the National Academy of Sciences of the United States of America. 2015; 112(18):5720–5725. DOI: 10.1073/pnas.1502111112 [PubMed: 25901323]

16. Pajerowski JD, Dahl KN, Zhong FL, Sammak PJ, Discher DE. Physical plasticity of the nucleus in stem cell differentiation. Proceedings of the National Academy of Sciences of the United States of America. 2007; 104(40):15619–15624. DOI: 10.1073/pnas.0702576104 [PubMed: 17893336]

17. Lammerding J, et al. Lamin A/C deficiency causes defective nuclear mechanics and mechanotransduction. Journal of Clinical Investigation. 2004; 113(3):370–378. DOI: 10.1172/ JCI19670 [PubMed: 14755334]

18. Chancellor TJ, Lee J, Thodeti CK, Lele T. Actomyosin tension exerted on the nucleus through nesprin-1 connections influences endothelial cell adhesion, migration, and cyclic strain-induced reorientation. Biophysical Journal. 2010; 99(1):115–123. DOI: 10.1016/j.bpj.2010.04.011 [PubMed: 20655839]

19. Neelam S, Dickinson RB, Lele TP. New approaches for understanding the nuclear force balance in living, adherent cells. Methods. 2016; 94:27–32. DOI: 10.1016/j.ymeth.2015.06.014 [PubMed: 26115785]

SUMMARY

In this protocol, we describe a micropipette method to directly apply a controlled force to the nucleus in a living cell. This assay allows interrogation of nuclear mechanical properties in the living, adherent cell.
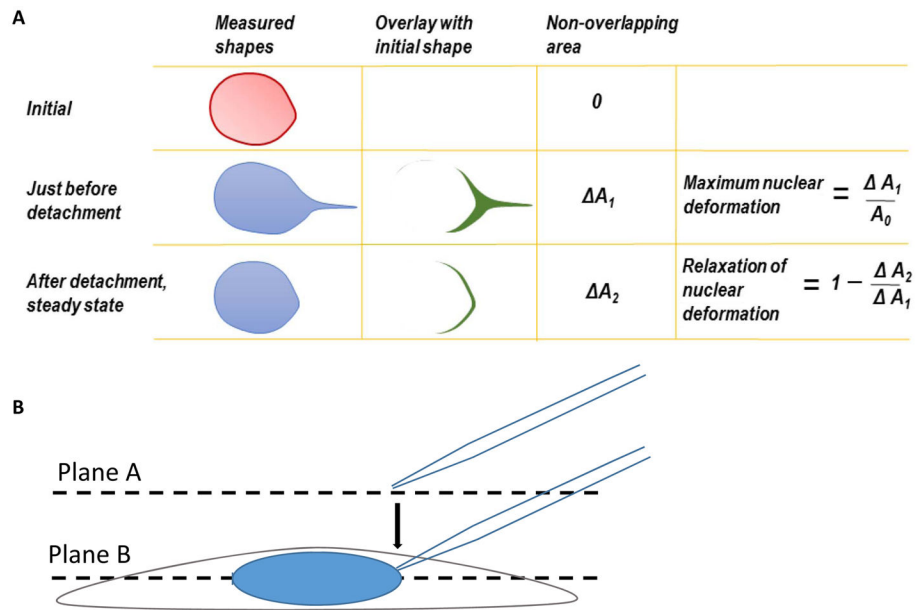
Figure 1. Nuclear Deformation and Microscope Focusing

A. Maximum nuclear deformation and relaxation of nuclear deformation. Before calculating maximum nuclear deformation, the back edges of the nuclear shapes were first coincided to correct for the translation of deformed nucleus. The shape of the nucleus at the moment of micropipette tip detachment was overlaid on the initial nuclear shape before pulling. The difference in area between the two shapes was measured as A_1. The maximum nuclear deformation was defined as A_1 divided by the original nuclear area. Similarly, a second parameter, A_2, may be defined by overlaying the final steady state nuclear shape after micropipette detachment on the original nuclear shape. B. Focus the cell at plane A and then move the focal plane up to plane B to find the micropipette tip. During imaging, the micropipette was translated to the right (direction of orange arrow). This figure has been modified from Neelam *et al.*[15].
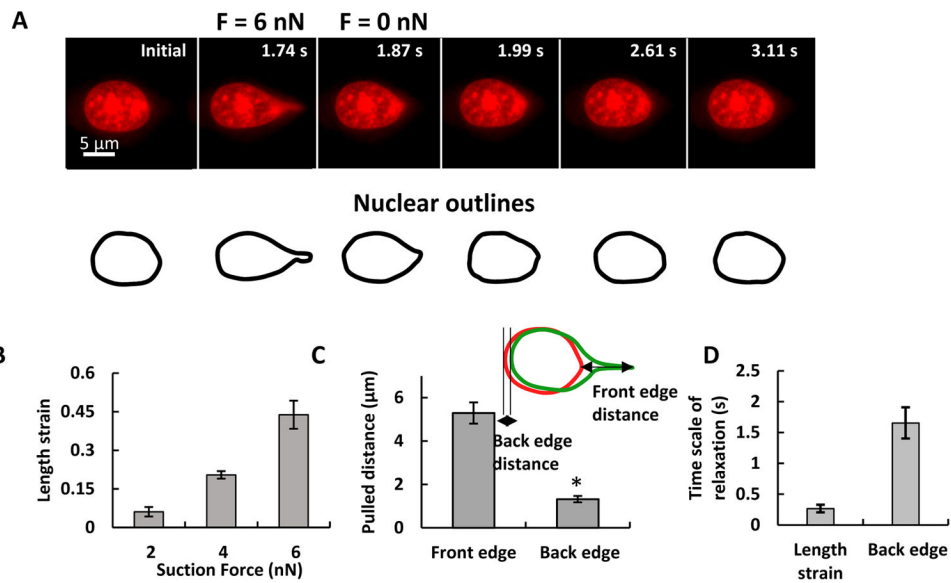
Figure 2. Characterization of the Nuclear Deformation

Deformation and displacement of the nucleus in a living, adherent cell by the DFP. A NIH 3T3 fibroblast nucleus was pulled with 6 nN force. The images show the nuclear shape at the indicated time. Scale bar: 5 μm B. Nuclear deformation was quantified by length strain. The nuclear deformation increased with applied forces. Error bars indicate standard error of the mean (SEM); n>6. C. The displacement at the leading edge is larger than the displacement at the trailing edge. D. The length strain relaxation is much faster than back edge relaxation. *P < 0.5; error bars indicate SEM; n=10. This figure has been modified from Neelam *et al.*[15].
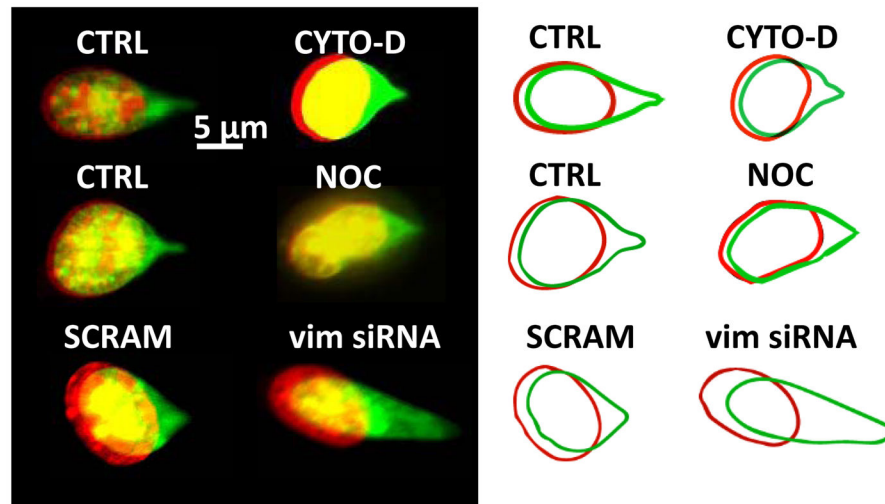
Figure 3. Fluorescent Images of the Nuclear Deformation
DFP was used to determine the contribution of cytoskeletal forces to nuclear deformation. The nucleus was stained with SYTO 59 dye. Fluorescent images show the overlay of the nucleus before (red, pseudo-color) and after (green, pseudo-color) at the indicated condition. CTRL, control cells; CYTO-D, cells treated with cytochalasin-D; NOC, cells treated with nocodazole; SCRAM, cells transfected with scrambled siRNA; vim siRNA, cells transfected with siRNA targeting vimentin. This figure has been modified from Neelam *et al.*[15].